Phe[120] contributes to the regiospecificity of cytochrome P450 2D6: mutation leads to the formation of a novel dextromethorphan metabolite

Jack U. FLANAGAN*, Jean-Didier MARÉCHAL†‡, Richard WARD‡, Carol A. KEMP†‡, Lesley A. McLAUGHLIN*, Michael J. SUTCLIFFE†‡, Gordon C. K. ROBERTS‡, Mark J. I. PAINE* and C. Roland WOLF*[1]

*Biomedical Research Centre, University of Dundee, Ninewells Hospital and Medical School, Dundee DD1 9SY, U.K., †Department of Biochemistry and Department of Chemistry, University of Leicester, University Road, Leicester LE1 7RH, U.K., and ‡Biological NMR Centre and Department of Biochemistry, University of Leicester, PO Box 138, University Road, Leicester LE1 9HN, U.K.

Although the residues that determine the preference of CYP2D6 (cytochrome P450 2D6) for compounds containing a basic nitrogen are well characterized, the contribution of other active site residues to substrate binding and orientation is less well understood. Our structural model of CYP2D6 identifies the aromatic residue Phe[120] as a likely major feature of the active site. To examine the role of Phe[120], mutants of CYP2D6 in which this residue has been substituted by alanine, leucine, tyrosine, serine, histidine, tryptophan or methionine residues have been prepared in bacterial membranes co-expressing human cytochrome NADPH cytochrome P450 oxidoreductase. The mutants have been characterized using the prototypical bufuralol 1′ hydroxylase and dextromethorphan O- and N-demethylase activities of CYP2D6. Larger effects on K_m values are observed for dextromethorphan O-demethylation than for bufuralol 1′ hydroxylation, indicating that the Phe[120] side chain is more important in dextromethorphan than in bufuralol binding. A role for this side chain in determining the regiospecificity of substrate oxidation was indicated by changes in the relative rates of O- and N-demethylation of dextromethorphan and, notably, by the formation of 7-hydroxy dextromethrophan, a novel dextromethorphan metabolite, in mutants in which it had been substituted. Computational studies of dextromethorphan binding to the active site of the Phe[120] → Ala mutant were carried out to throw light on the way in which the removal of this side chain leads to different modes of ligand binding.

Key words: cytochrome P450, cytochrome P450 2D6 (CYP2D6), dextromethorphan, drug metabolism, ligand-binding property, mutagenesis.

INTRODUCTION

Cytochromes P450 are a large superfamily of haem-containing mono-oxygenases responsible for the oxidative metabolism of an extremely wide variety of substrates. Human CYP2D6 (cytochrome P450 2D6) is one of the most important members of this family due to its central role in the metabolism of many drugs in common clinical use [1], including opioids, antidepressants, neuroleptics and various cardiac medications. *CYP2D6* is polymorphic in the human population, giving rise to significant inter-individual and ethnic differences in drug metabolism [2,3]. The 'poor metabolizer' phenotype that arises from the absence of functional CYP2D6 results in impaired drug oxidation reactions [4] and may be linked to altered disease susceptibility [5,6].

CYP2D6 metabolizes a diverse group of compounds, but several key structural features of its substrates have been identified (for example, reviewed in [7]), the best known of which is a basic nitrogen atom present in the majority of CYP2D6 substrates between 5 and 10 Å (1 Å ≡ 0.1 nm) from the site of metabolism. However, the fact that CYP2D6 shows activity towards substrates, such as progesterone [8], pregnenolone [9] and spirosulphonamide [10], that do not contain a basic nitrogen, indicates that this is not an absolute requirement. An apparent increase in active site volume by substitution of Phe[483] is sufficient to allow CYP2D6-mediated testosterone metabolism [11]. Furthermore, the enzyme can catalyse N-dealkylation reactions of substrates, such as deprenyl [12], amitriptyline [13], methamphetamine [14], the neurotoxin 1-methyl-4-phenyl-1,2,3,6-tetrahydro pyridine [15] and dextromethorphan [16], a commonly used antitussive.

The acidic residues that influence CYP2D6 substrate selectivity with respect to basic nitrogen-containing compounds have been well characterized [10,17–21]. We have recently described a structural model of CYP2D6 [22] that identified the carboxylate-containing residues Glu[216] and Asp[301] as key sites of interaction between the CYP2D6 active site and the basic nitrogen of the substrate [21]. However, little is known about the contribution of other active site residues to substrate binding and orientation. In addition to the basic nitrogen, most CYP2D6 ligands contain a planar hydrophobic moiety [7]. Our model shows that an aromatic residue, Phe[120] (located in the B′–C loop), occupies a position close to the haem, where it would be expected to have a major influence on substrate binding (Figure 1). We have now used site-directed mutagenesis and molecular modelling to investigate the role of this residue in substrate binding and catalysis. Our results show that the aromatic side chain of Phe[120] does affect the orientation of molecules in the active site of CYP2D6, and hence plays an important role in controlling the regioselectivity of substrate oxidation.

EXPERIMENTAL

Chemicals

TB (Terrific broth), chloramphenicol, δ-aminolevulinic acid, glucose 6-phosphate, $NADP^+$, PMSF, sodium dithionite, cytochrome *c*, dextromethorphan and diclofenac were all purchased from Sigma (Poole, Dorset, U.K.). Ampicillin was obtained from Beecham Research (Welwyn Garden City, U.K.) and isopropyl

Abbreviations used: CYP2D6, cytochrome P450 2D6; F120Y etc., Phe[120] → Tyr replacement etc.; P450 reductase, NADPH cytochrome P450 oxidoreductase; TB, Terrific broth.

[1] To whom correspondence should be addressed (e-mail roland.wolf@cancer.org.uk).

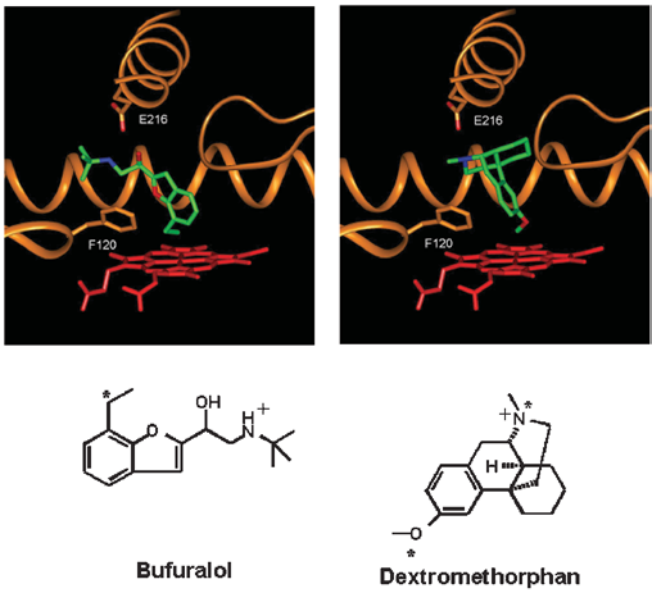

Figure 1 Model of the active site of CYP2D6 showing the predicted location of the Phe^{120} aromatic side-chain

Bufuralol (left-hand panel) and dextromethorphan (right-hand panel) are shown docked in the position corresponding to the major route of metabolism by wild-type CYP2D6. In each case the site of metabolism is positioned above the iron atom of the haem, and the basic nitrogen atom of the substrate forms a salt bridge with the carboxylate group of residue Glu^{216} located in the F-helix. The structures of bufuralol and dextromethorphan are shown with the sites of metabolism indicated by an asterix. The + indicates the basic N atom.

β-D-thiogalactoside from Melford Laboratories (Ipswich, U.K.). Glucose 6-phosphate dehydrogenase (type VII) was from Roche Molecular Biochemicals (Lewes, East Sussex, U.K.). HPLC grade solvents were purchased from Rathburn Chemicals (Walkerburn, Peeblesshire, Scotland, U.K.), and HPLC columns from Agilent (Crawford Scientific, Strathaven, Lanarkshire, Scotland, U.K.). DNA modifying enzymes were obtained from Gibco BRL (Paisley, Renfrewshire, Scotland, U.K.) and Promega (Chilworth, Southampton, U.K.). Dextrorphan, 3-methoxy morphinan, 3-hydroxymorphinan, bufuralol and 1′-hydroxy bufuralol were purchased from Ultra Fine Chemicals (Manchester, U.K.). All other chemicals were from BDH (Poole, Dorset, U.K.). Library efficient competent *Escherichia coli* JM109 were purchased from Promega.

Mutagenesis

The isolation of the cDNAs and construction of expression plasmids ompA CYP2D6(His$_7$) (pB81) and pJR7 [human P450 reductase (NADPH cytochrome P450 oxidoreductase)] have been described previously [11,23,24]. Site-directed mutagenesis was performed using the single-stranded DNA template method [25] using pB81 as a template, the *dut*$^-$ *ung*$^-$ *E. coli* strain CJ236 and the mutating oligonucleotide. A list of the reverse compliment oligonucleotides used with the altered nucleotides underlined is as follows: F120Y (Phe^{120} → Tyr replacement), 5′-ATAGCGCGCCAGGTACACCCCTTGGGA-3′; F120A, 5′-ATAGCGCGCCAGGGCCACCCCTTGGGA-3′; F120H, 5′-GCGCGCCAGGTGCACCCCTTGGGA-3′; F120W, 5′-GCGCGCCAGCCACACCCCTTGGGA-3′; F120S, 5′-GCGCGCCAGGGACACCCCTTGGGA-3′; F120L, 5′-GCGCGCCAGCAACACCCCTTG-3′; F120M, 5′-GCGCGCCAGCATCACCCC-3′. The presence of the desired mutations was confirmed by automated DNA sequencing.

Co-expression of CYP2D6 and P450 reductase in *E. coli*

Single colonies of co-transformants were selected on Luria–Bertani plates supplemented with 50 μg/ml ampicillin and 25 μg/ml chloramphenicol. For protein expression, 250 ml of TB supplemented with 50 μg/ml ampicillin contained in a 2 litre flask was inoculated at 1:50 with an overnight culture grown at 37 °C in Luria–Bertani broth supplemented with 50 μg/ml ampicillin and 25 μg/ml chloramphenicol, and grown at 30 °C. When the D_{600} reached 0.45 to 0.5, δ-aminolevulinic acid was added to a final concentration of 0.5 mM, and protein expression was induced at D_{600} 0.9 to 1.0 by the addition of isopropyl β-D-thiogalactoside to a final concentration of 1 mM. Cells were harvested by centrifugation at 4500 ***g*** at 4 °C for 25 min using a H6000A rotor in a Sorvall RC3C centrifuge. The pellet was resuspended in ice-cold 1 × TSE (50 mM Tris Acetate, pH 7.6, 250 mM sucrose, 0.25 mM EDTA) [26] at 100 ml/litre of starting culture, treated with 50 μg/ml lysozyme for 60 min at 4 °C, repelleted, and resuspended in ice-cold 1 × TSE for storage at −70 °C. Bacterial membranes were isolated according to the method of Renaud et al. [26]. Whole cells were thawed in the presence of the protease inhibitors aprotinin and leupeptin at a final concentration of 1 μg/ml, and PMSF to 1 mM final concentration. The cells were subsequently sonicated and centrifuged for 20 min at 12000 ***g*** at 4 °C using an SS-34 rotor in a Sorvall RC-5B centrifuge. Bacterial membranes were isolated from the supernatant by centrifugation for 50 min at 180000 ***g*** at 4 °C using a T-1250 rotor in an OTD 65B Sorvall Ultracentrifuge. The membrane pellet was resuspended in ice-cold 1 × TSE and stored frozen at −70 °C.

Enzyme assays

Before use, membranes were characterized with respect to recombinant CYP content, as estimated by Fe^{2+}-CO versus Fe^{2+} difference spectra [27], and human cytochrome P450 reductase content, as estimated by cytochrome *c* reductase activity. Reductase assays were carried out at 25 °C as described previously [21], in 0.3 M potassium phosphate pH 7.7 using final concentrations of 50 μM cytochrome *c* and 50 μM NADPH.

CYP content for all enzyme assays was standardized at 5 pmol per 100 μl of final reaction volume. Routinely, an NADPH-generating system was used to maintain a continual source of NADPH throughout the course of the reaction; this consisted of $NADP^+$, glucose-6-phosphate and glucose-6-phosphate dehydrogenase at final concentrations of 0.001 mM, 0.025 mM and 1 unit/ml respectively. All reactions were performed in 50 mM potassium phosphate, pH 7.4, at 37 °C in opaque Eppendorf tubes. After pre-incubation at 37 °C for 3 min, reactions were initiated by the addition of the NADPH-generating system.

Dextromethorphan O- and N-demethylation

Owing to the differences in reaction rate between the mutant isoforms under investigation, incubation times varied. The wild-type, F120A and F120H reactions were incubated for 6 min, whereas those of F120L and F120H were incubated for 15 min. Reactions were quenched by the addition of ice-cold methanol and 60 % $HClO_4$ to final concentrations of 33 % and 1 % respectively, and incubated on ice for 10 min prior to centrifugation at 16000 ***g*** for 5 min to remove particulate material. Routinely, 100 μl of the reaction supernatant was assayed for the presence of the metabolites dextrorphan and 3-methoxy morphinan (the O- and

N-demethylation products of dextromethorphan respectively) using reversed-phase HPLC. Dextrorphan, was separated using an Agilent Technologies Hypersil BDS-C18 column (5 μm pore size; 4.6 mm × 250 mm) at 25 °C with acetonitrile (22 %) and 0.1 M ammonium acetate, pH 5.0 (78 %), run isocratically at a flow rate of 1 ml/min. Using the same column matrix, 3-methoxy morphinan was separated by a mobile phase of acetonitrile (32 %) and 0.1 M ammonium acetate, pH 5.0 (68 %), run isocratically at 1 ml/min. Both dextromethorphan metabolites were detected using $\lambda_{excitation} = 252$ nm and $\lambda_{emission} = 302$ nm.

Bufuralol 1′ hydroxylation

The wild-type, F120A and F120H reactions were incubated for 2 min, whereas those of F120L and F120H were incubated for 8 min. Reactions were quenched by the addition of 60 % $HClO_4$ to a final concentration of 5 %, and incubated on ice for 10 min prior to centrifugation at 16000 ***g*** for 5 min to remove particulate material. Routinely, 20 μl of the reaction supernatant was assayed using reversed-phase HPLC for the presence of the metabolite. 1′-Hydroxy bufuralol was separated using a Hypersil ODS column (5 μm; 125 mm × 4.0 mm), with 100 mM ammonium acetate, pH 5, (Buffer A) and acetonitrile (Buffer B) applied as a step gradient at a flow rate of 1.0 ml/min. The gradient profile was: 0 min, A/B, 73 %/27 %; 11.3 min, A/B 60 %/40 %; 12.3 min, A/B, 49 %/51 %; 13.3 min, A/B, 73 %/27 % (all v/v). The fluorescent metabolite 1′ hydroxy bufuralol was detected using $\lambda_{excitation} = 252$ nm and $\lambda_{emission} = 302$ nm.

Analysis of novel oxidative product

NMR spectroscopy

The novel metabolite was purified by HPLC using the column and elution solvent described above for separation of dextrorphan. The solvent was removed by freeze drying and the metabolite was dissolved in ^2H_2O. ^{1}H-NMR spectra were obtained at 500 MHz, and assigned by using two dimensional ^{1}H-^{1}H COSY and NOESY experiments. Proton resonance assignments: δ_H 7.18 (1 H, d, C1-H, J 8.6 Hz), 6.96 (1 H, d, C4-H, J 2.6 Hz), 6.89 (1 H, dd, C2-H, $J = 2.6$ and 8.4 Hz), 3.98 (1 H, m, C7-H), 3.77 (3 H, s, O-CH_3), 3.58 (1 H, m, C9-H), 3.16–3.10 (3 H, m, C10-H_2 and C16-H), 2.84 (3 H, s, N-CH_3), 2.68 (1 H, m, C16-H), 2.32 (1 H, m, C14-H), 2.25 (1 H, m, C5-H), ~1.85 (C15-H), 1.71 (1 H, m, C5-H), 1.66–1.54 (3 H, m, C6-H, C8-H and C15-H), 1.42 (1 H, m, C6-H), 1.27 (1 H, m, C8-H). The resonance of one C15-proton appears under the signal at 1.85 ppm which arises from an acetate impurity.

Molecular modelling

The structural models of CYP2D6 were produced as described previously [22]. In brief, the models were generated by comparative modelling using Modeller [28] with five structural templates: P450s cam, terp, eryF, BM3 and 2C5. They were validated by comparison of their stereochemical and non-bonded properties with those of the experimental structures of the five templates used in the modelling. The F120A mutant structure was generated by replacing the phenyl ring of Phe[120] by a hydrogen atom, with no further optimization.

Docking Studies

Docking calculations have been carried out for dextromethorphan binding to the CYP2D6 wild-type and CYP2D6 F120A mutant models using the program GOLD version 2.0 [29–31]. Prior to docking, the structure of dextromethorphan was downloaded from the ChemId plus database (http://chem.sis.nlm.nih.gov/chemidplus) and energy minimized using the program Sybyl version 6.8 [32]. Docking solutions were generated defining the active site cavity as a sphere of 20 Å radius centred on the Fe atom of the haem. Ten solutions were generated for each docking experiment and ranked according to the Goldscore scoring function. The best solution (highest Goldscore value) was used for further more detailed analysis.

In order to generate orientations of dextromethorphan in the active site which would be consistent with the experimental observations of the production of 3-methoxy morphinan (*N*-demethylation) and 7-hydroxy dextromethrophan (7-hydroxylation) appropriate distance constraints were incorporated in the docking calculations, as described in the Results section.

RESULTS

Site-directed mutagenesis of F120

A series of CYP2D6 mutants were constructed in which Phe[120] was replaced by other aromatic residues (tryptophan, tyrosine), by non-aromatic hydrophobic residues (leucine, methionine), by polar residues (serine, histidine) and by alanine. The F120M and F120W mutants failed to form spectroscopically detectable P450. The yields of the other mutant P450s were: F120A, 263 nmol/l of *E. coli* culture; F120L, 363 nmol/l; F120H, 210 nmol/l; F120Y, 252 nmol/l; F120S, 463 nmol/l; all of which compared favorably with 300 nmol/l for wild-type CYP2D6. P450 reductase levels were between 30 and 179 nmol of cytochrome *c* reduced/min per mg of *E. coli* membrane. When measuring the P450 content of the *E. coli* membranes, it was observed that the P450 peaks of the F120A and F120Y mutants started to convert to P420 within a few minutes, indicating they are less stable than the other mutant isoforms during P450(Fe^{2+})-CO versus P450(Fe^{2+}) difference spectroscopy. Due to the extremely low activity and instability of the F120Y mutant, no further analysis of this mutant was performed.

Kinetic properties of the wild-type CYP2D6 and Phe[120] mutant isoforms

Characterization of enzyme activities was carried out using the 1′-hydroxylation of bufuralol and the O-demethylation of dextromethorphan, two prototypical CYP2D6 substrates that contain planar ring structures and a basic nitrogen atom (Figure 1). The kinetic parameters are presented in Table 1. The removal of the Phe[120] aromatic side chain by substitution with alanine

Table 1 Kinetic parameters for bufuralol 1′-hydroxylation and dextromethorphan O-demethylation by wild-type and mutant CYP2D6

Assays were performed in triplicate as described in the Experimental section. The error values shown are S.D., calculated from fitting the Michaelis–Menten equation to the data.

	Bufuralol 1′-hydroxylation		Dextromethorphan O-demethylation	
CYP2D6	K_m (μM)	k_{cat} (min^{-1})	K_m (μM)	k_{cat} (min^{-1})
Wild-type	4.1 ± 2.5	4.1 ± 0.9	1.0 ± 0.3	3.0 ± 0.5
F120A	2.7 ± 1.0	3.1 ± 0.9	1.0 ± 0.1	6.6 ± 0.9
F120L	5.1 ± 1.4	0.4 ± 0.1	32 ± 3.3	1.9 ± 0.3
F120H	10.3 ± 1.6	4.3 ± 1.2	10 ± 1.2	5.3 ± 0.9
F120S	3.3 ± 0.8	0.5 ± 0.2	16 ± 1.5	1.7 ± 0.2

(F120A) had very little effect on the K_m for either substrate. In contrast, replacement of Phe[120] with leucine, serine or histidine caused 10- to 32-fold increases in K_m with respect to dextromethorphan O-demethylase activity, whereas only the serine substitution caused a significant (though modest, 2.5-fold) change in K_m for the bufuralol 1′-hydroxylase activity.

In most cases the effect of the substitution of Phe[120] on k_{cat} values for bufuralol 1′-hydroxylation or dextromethorphan O-demethylation was modest, $\leqslant$ 2.2-fold, although the leucine and serine substitutions led to 8- to 10-fold decreases in k_{cat} values for bufuralol 1′-hydroxylation. The effects of substitution at this position are thus dependent on the nature of the side chain and the nature of the substrate.

It is particularly notable that the F120A mutant is at least as active against both substrates as the wild-type enzyme, demonstrating that the phenyl ring of Phe[120] is not essential for substrate binding. However, studies of the products of dextromethorphan metabolism by this mutant show that Phe[120] does play an important role in determining the orientation of the substrate in the active site, and hence in the regiospecificity of the enzyme.

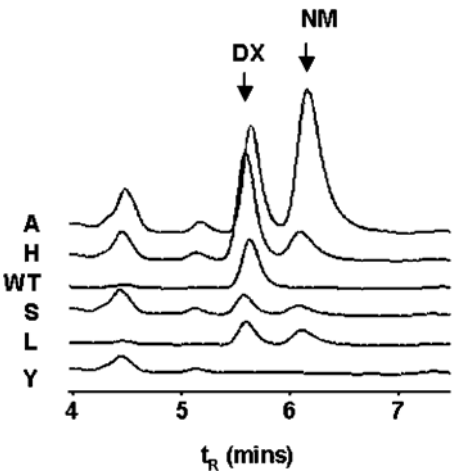

Figure 2 HPLC chromatograms illustrating the separation of the dextromethorphan O-demethylated product, dextrorphan, for the wild-type (WT) and mutant CYP2D6 isoforms used in this study

Reactions were carried out as described in the Experimental section. The O-demethylation product, dextrorphan, is labelled DX. NM is the novel metabolite peak. The plot represents reactions carried out at a final concentration of 1 mM dextromethorphan. The traces are in descending order according to the amount of peak NM produced.

Dextromethorphan metabolism

The major pathway of dextromethorphan metabolism by CYP2D6 is O-demethylation, with the formation of dextrorphan. However, CYP2D6 can also catalyse demethylation at the basic nitrogen to produce 3-methoxy morphinan, the relative rates of the two reactions being dependent on substrate concentration [16]. Comparison of the relative rates of O- and N-demethylation of dextromethorphan by wild-type CYP2D6 and the mutants is shown in Table 2. Substitution of the Phe[120] side chain with alanine leads to some change in the relative rates of these two reactions, the direction of the change being dependent on the substrate concentration. Thus at 0.1 mM dextromethorphan the 3-methoxy morphinan/dextrorphan ratio is 0.44 for CYP2D6 F120A compared with 0.25 for the wild-type enzyme, whereas at 1.0 mM substrate the ratio is 1.0 for the mutant compared with 3.1 for the wild-type. Interestingly, in addition to these changes in the ratio of the rates of formation of known metabolites, the HPLC traces for the separation of dextrorphan (Figure 2), showed the formation, by F120A and several other mutants but not by the wild-type, of a peak eluting at approx. 6.5 min corresponding to a novel metabolite of dextromethorphan. This peak is produced in the presence of catalase and superoxide dismutase (up to 1000 units and 16 μg respectively), and thus represents a *bona fide* primary oxidation product of dextromethorphan. The novel metabolite was purified by HPLC, and analysed by ^{1}H NMR. The spectrum is generally well resolved, and was readily assigned on the basis of ^{1}H–^{1}H COSY (Figure 3) and NOESY spectra; the assignments are indicated in Figure 3 and the chemical shifts and coupling constants are listed in the Experimental section. Comparison with the spectrum of dextromethorphan immediately showed that the N-methyl, O-methyl and aromatic resonances are identical, ruling out these parts of the molecule as sites of metabolism in this product. A new resonance is observed at 3.98 p.p.m., a chemical shift consistent with a -C*H*OH- moiety. The connectivities in the COSY spectrum to the two C6 protons and the two C8 protons (and hence through to C14-H and C9-H) allow this to be assigned to C7-H. The novel metabolite is thus identified as 7-hydroxy dextromethrophan.

The novel 7-hydroxy dextromethrophan was also produced by all other mutants, but at much lower levels than the F120A substitution. As shown in Table 2, the metabolism of dextromethorphan by F120A leads to the formation of three metabolites (dextrorphan, 3-methoxy morphinan and 7-hydroxy dextromethrophan) in comparable amounts; at 1 mM substrate, the new metabolite 7-hydroxy dextromethrophan is the major product. These observations clearly suggest that the removal of the aromatic side chain of Phe[120] from the active site cavity has removed

Table 2 Regiospecificity of dextromethorphan metabolism by wild-type and mutant CYP2D6

The activities are derived from the mean and S.D. of three separate reactions. Assays were performed as described in the Experimental section. DX, dextrorphan; 3MM, 3-methoxy morphinan; 7-HD, 7-hydroxy dextromethorphan; N.D, product not detectable.

Dextromethorphan (mM) . . .	Dextromethorphan metabolism (peak area/min)					
	0.1			1.0		
	DX	3MM	7-HD	DX	3MM	7-HD
Wild-type	7.3 ± 1.4	1.8 ± 0.1	N.D.	6.4 ± 0.03	20 ± 0.6	N.D.
F120A	16 ± 0.2	7.1 ± 0.4	3.6 ± 0.01	14 ± 0.5	14 ± 0.4	27 ± 0.1
F120L	2.8 ± 0.1	2.0 ± 0.1	N.D.	2.9 ± 0.2	14 ± 0.5	2.7 ± 0.5
F120H	13 ± 0.1	7.0 ± 0.7	N.D.	13 ± 0.1	20 ± 0.9	4.8 ± 0.2
F120S	2.3 ± 0.03	5.5 ± 0.4	N.D.	2.3 ± 0.04	5.1 ± 0.3	1.5 ± 0.1

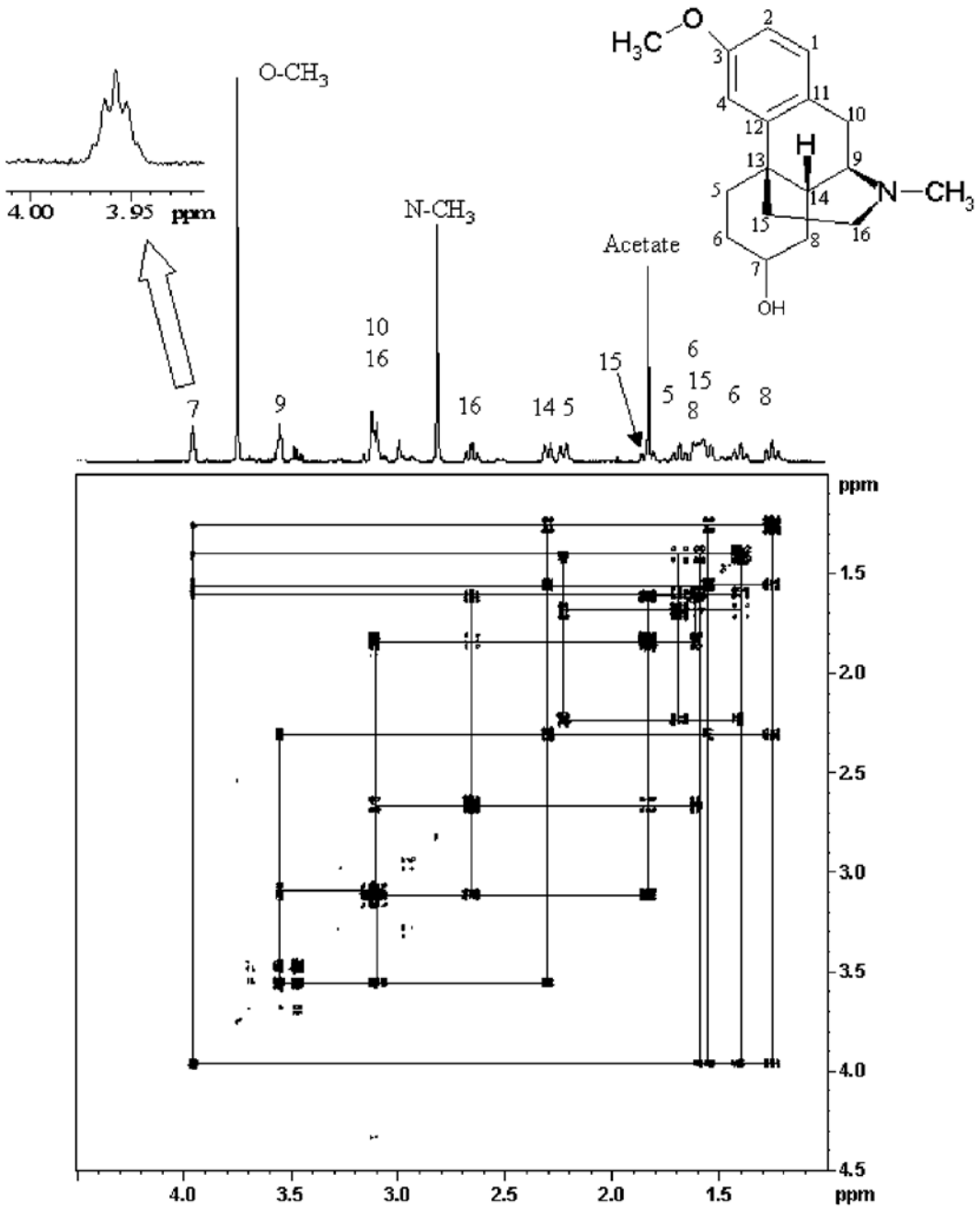

Figure 3 ^{1}H NMR spectra of the novel metabolite

The aliphatic regions of the one-dimensional ^{1}H and two-dimensional ^{1}H-^{1}H COSY spectra are shown. NMR data were collected at 500 MHz and 300 K using a sample of the novel metabolite dissolved in $^{2}H_2O$. The resonance assignments are shown on the one-dimensional spectrum, and key connectivities on the COSY spectrum. The 7-hydroxy dextromethorphan structure with carbons numbered is shown in the upper right. An insert (upper left) shows an expansion of the resonance of the C7-H to reveal its fine structure.

a steric constraint on ligand binding, allowing the substrate to bind in several different orientations.

The effect of conservative substitutions with tyrosine or tryptophan cannot be tested, since neither mutant produced stable or active P450. Instead, we compared the products formed by the F120A mutant with the artificial oxygen and electron donors cumene hydroperoxide (CuOOH; [10]), which contains a benzene ring structure, or H_2O_2, which does not. As shown in Figure 4, dextrorphan is produced by both wild-type and F120A in the presence of either peroxide, but 7-hydroxy dextromethrophan is produced only with H_2O_2, not CuOOH. This clearly suggests that the binding of a bulky (aromatic) group into the active site of the F120A mutant restricts the orientation and mobility of dextromethorphan in the active site in a way analogous to the effect of the Phe[120] side chain in the wild-type enzyme.

Dextromethorphan-docking studies

To further study the differences between wild-type CYP2D6 and CYP2D6 F120A mutant, molecular docking studies were

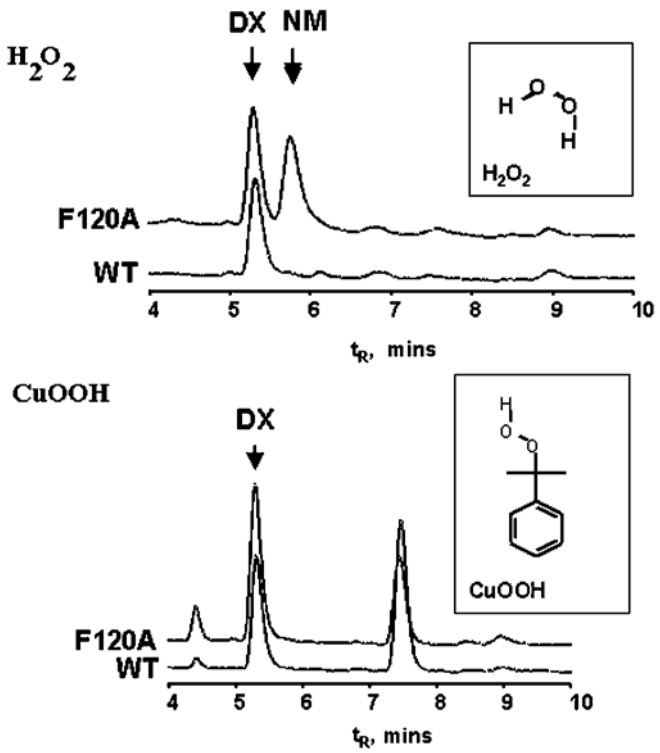

Figure 4 HPLC chromatograms illustrating the effect of H_2O_2 and CuOOH on dextromethorphan metabolism by the wild-type and F120A isoforms

HPLC traces are shown from reactions carried out with 1 mM dextromethorphan using H_2O_2 or CuOOH. Dextrorphan (DX) and novel metabolite (NM) peaks are indicated. The insets show structures of H_2O_2 and CuOOH. Reactions were carried out as described in the Experimental section. Stock peroxide oxygen donor systems of 1 mM CuOOH and 500 mM H_2O_2 were made up in 100 % methanol and used at final concentrations of 0.01 mM and 5 mM respectively.

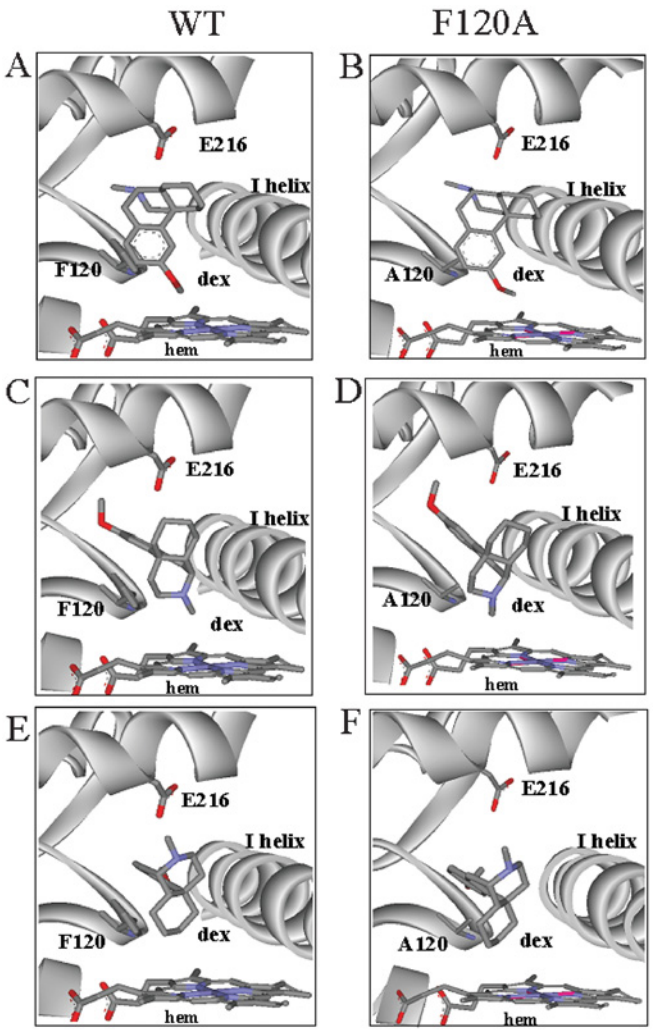

Figure 5 Docking of dextromethorphan into the CYP2D6 wild-type and F120A mutant active sites

The left-hand column shows the results of docking dextromethorphan into the wild-type model, and the right-hand column the results of docking it into the F120A mutant model. (**A** and **B**) Best solutions for dextromethorphan binding without constraint; mode of binding corresponding to O-demethylation. (**C** and **D**) Best solutions for dextromethorphan binding with the Fe–C7 distance constrained; mode of binding corresponding to N-demethylation. (**E** and **F**) Best solutions for dextromethorphan binding with the Fe–C7 distance constrained; mode of binding corresponding to 7-hydroxylation. The positions of the haem (hem), dextromethorphan (dex), and side chains Phe^{120}, Ala^{120} and Glu^{216} in relation to the I-helix are shown.

performed. Three different modes of binding suggested by the experimental results have been studied, corresponding to the production of dextrorphan (O-demethylation mode), 3-methoxy morphinan (N-demethylation mode) and 7-hydroxy dextromethorphan (7-hydroxylation mode).

The structural model of CYP2D6 was produced as described previously [22], and the model of the F120A mutant was produced by making the appropriate modification to the side chain, with no further optimization. Dextromethorphan was docked into both wild-type CYP2D6 and F120A models using the program GOLD [29–31]; analysis of the results revealed that in all the low energy solutions dextromethorphan adopts an orientation suitable for O-demethylation, with the methoxy group close to the haem. Figures 5(A) and 5(B) show the energetically most favourable solutions for both wild-type and mutant CYP2D6, and their energies are given in Table 3. These energies are very similar ($S_{TOT} = 49.0$ and 47.6 for wild-type and F120A respectively), although this comparison should be made with some caution since the corresponding three-dimensional structures are not exactly the same. These values are in general agreement with the relatively high binding affinity of dextromethorphan observed experimentally ($K_m = 1.0\ \mu M$ for both wild-type and F120A CYP2D6, Table 1). No significant structural differences are observed between these models of dextromethorphan binding to wild-type and F120A CYP2D6 (Figures 5A and 5B). For example, both solutions present a good hydrogen bond interaction between the basic nitrogen of dextromethorphan and one of the

Table 3 Energy scores from docking dextromethorphan into models of wild-type CYP2D6 and the F120A mutant

The scores were obtained with the program Gold version 2.0. S_{TOT} corresponds to the total Goldscore. S_{CONS} correspond to the part of the total Goldscore (S_{TOT}) produced by the constraint penalty. DX, dextrorphan; 3MM, 3-methoxy morphinan; 7-HD, 7-hydroxy dextromethorphan.

Mode of binding . . .	Energy score		
	DX	3MM	7-HD
Wild-type			
S_{TOT}	49.02	42.15	33.65
S_{CONS}	0.00	− 0.43	− 3.89
F120A			
S_{TOT}	47.58	43.10	36.99
S_{CONS}	0.00	− 0.13	− 1.37

O_γ atoms of Glu[216], whose role in the CYP2D6 active site has been described previously [21]. It appears therefore that removing the aromatic moiety of Phe[120] from the CYP2D6 binding site does not alter the ability of dextromethorphan to bind in an orientation appropriate for O-demethylation, consistent with the observation that the kinetic parameters for this reaction are scarcely changed by the F120A substitution.

Unrestrained dockings were unable to reproduce binding modes of dextromethorphan corresponding to N-demethylase and 7-hydroxylase activities; thus further studies aimed at understanding the whole range of CYP2D6 activity have been carried out by incorporating structural restraints. First, a restraint was applied to the C17–Fe distance, requiring this distance to remain between 1.0 and 3.5 Å with a penalty force constant of 1.0 [33]. In all the solutions generated in the presence of this constraint, dextromethorphan adopts an orientation in the active site consistent with N-demethylation. The solutions with the lowest energies for this binding mode are shown in the Figures 5(C) and 5(D) and their energies are given in Table 3. For both wild-type and F120A CYP2D6, the energies of the best solutions correspond to good binding affinities ($S_{TOT} = 42.2$ and 43.1 for wild-type and F120A respectively), but are less energetically favourable than the complexes in which the orientation of the substrate corresponds to O-demethylation. The breakdown of the Goldscore values shows that the constraints are well satisfied in both the wild-type and F120A ($S_{CONS} = -0.13$ and -0.43 respectively). Only very subtle structural differences are observed between the mutant and wild-type for this docking orientation. The main difference is that in the wild-type binding site, the aromatic ring of Phe[120] clashes with the substrate and prevents the ligand from getting as close to the haem iron, as it can in the mutant binding site (Figures 5C and 5D). The absence of the aromatic moiety of Phe[120] does not lead, however, to a significant modification in the binding orientations. These results are consistent with the experimental observation that N-demethylation is catalysed by both CYP2D6s, at rates less than or equal to the rate of O-demethylation, with the mutant catalysing N-demethylation somewhat faster than the wild-type at low substrate concentrations.

In order to investigate the binding mode of dextromethorphan which would lead to 7-hydroxylation, a restraint was applied to the C7–Fe distance, requiring it to remain between 1.0 and 3.5 Å, with a force constant of 1.0. In all the solutions generated in the presence of this constraint, dextromethorphan does indeed adopt an orientation in the active site consistent with 7-hydroxylation. The lowest energy docking solutions for both wild-type and F120A are shown in Figures 5(E) and 5(F) and their respective energies are given in Table 3. In this mode of binding the differences between wild-type and F120A are clearly more significant, in terms of both energy and structure, than those seen for the other orientations of dextromethorphan. First, the Goldscore values show that binding in this is less energetically favourable than in other orientations for both wild-type and F120A CYP2D6 ($S_{TOT} = 33.7$ and 37.0 respectively), and that this difference is clearly greater for the mutant enzyme. Furthermore, the Goldscore restraint penalty is almost three times higher in the wild-type than in the F120A enzyme ($S_{CONS} = -3.9$ and -1.4 in wild-type and F120A enzyme respectively). The docking calculations thus indicate that binding in the orientation appropriate for 7-hydroxylation is energetically more stable in the F120A mutant binding site than in the wild-type one. This energetic difference is reflected in significant differences in ligand–protein contacts between the wild-type and mutant model complexes. There are no clashes between the ligand and the protein in the model of the F120A complex, but in the wild-type complex clashes occur in two regions: between the N-methyl carbon of dextromethorphan and the Thr[215] side chain, and between the ring containing C7 of dextromethorphan and the Phe[120] side chain. The results of the docking calculations thus indicate that removal of the aromatic ring of Phe[120] does facilitate the binding of dextromethorphan in an orientation which leads to 7-hydroxylation.

DISCUSSION

We recently demonstrated important roles for two active site residues, Asp[301] and Glu[216], in determining substrate specificity in CYP2D6 [21]; both have a role in interacting with the basic nitrogen of substrates, but in addition Asp[301] appears to be involved in positioning the B–C loop. Further examination of our model points to residue Phe[120] in the B–C loop as potentially being important in substrate binding and this has now been explored further. Substitution of the aromatic residue by alanine had little effect on the K_m of either substrate, indicating that Phe[120] is not essential for substrate binding. However, it is clear that the Phe[120] side chain does influence substrate binding, as illustrated by the 30-fold increase in dextromethorphan K_m in the F120L mutant. The lack of effect on the K_m for bufuralol indicates that the role of this residue in binding is substrate dependent. In general, the effects of the mutants on the kinetic parameters were more pronounced with dextromethorphan, which may be related to its rigid structure.

Other CYP2D6 aromatic active site residues of Phe[481] and Phe[483], located in the β1–4 loop have also been proposed to aid ligand binding [34,35]. The location of this loop, defining the wall of the active site opposite that of the B′–C loop and Phe[120], implies a potential for a concerted or individual role for the aromatic residues in ligand orientation. Strikingly, an analogous situation has been illustrated with the determination of the CYP2C9 crystal structure in complex with its substrate warfarin [36]. Thus separate from the mechanisms that define the distinct substrate charge preferences observed for CYP2D6 and CYP2C9 respectively [37,38], various members of the CYP2 family appear to employ specific aromatic interactions as a common mechanism of ligand orientation.

While the F120A substitution produced no obvious decrease in the binding affinity of dextromethorphan, HPLC analysis of the metabolites showed changes in the regioselectivity of oxidation relative to the wild-type, with the appearance of a novel 7-hydroxylated product, 7-hydroxy dextromethrophan, being most prominent. Analysis of 7-hydroxy dextromethrophan production using peroxides as oxygen and electron donors showed that the bulky organic peroxide, CuOOH, did not support dextromethorphan 7-hydroxylation, whereas it was supported by H_2O_2, which lacks the bulky aromatic group. Computational studies of dextromethorphan binding by both wild-type and F120A mutant enzymes indicates that removal of the Phe[120] side chain allows the substrate closer to the haem iron in the N-demethylation orientation, as well as the ability to re-orient and allow novel substrate sites access to the haem. An analogous effect on substrate orientation has been observed in human CYP2C9 [39] and bacterial CYP102A1 [40] where phenylalanine residues equivalent to Phe[120] have been mutated.

Taken together, these results clearly illustrate an important role for Phe[120], located on the B′–C loop, in determining the regiospecificity of substrate oxidation by CYP2D6, thus helping to define the characteristic ligand-binding properties of this enzyme. For the future development of predictive models of the specificity of CYP2D6, it will be important to take into account the influential role of Phe[120] in substrate orientation along with

the roles of Glu^{216} and Asp^{301} in selecting for basic nitrogen compounds [19–21].

This work was funded by the Drug Metabolism Consortium (AstraZeneca, Aventis, Boehringer Ingelheim, CellTech Chiroscience, GlaxoSmithKline, Hoffmann-La Roche, Johnston and Johnston Pharmaceuticals, Merck Sharp and Dohme, Novartis, Novo Nordisk, Pfizer, Pharmacia and Wyeth).

REFERENCES

1 Smith, D. A. (1997) Pharmacokinetics and pharmacodynamics in toxicology. Xenobiotica **27**, 513–525
2 Eichelbaum, M., Spannbrucker, N., Steincke, B. and Dengler, H. J. (1979) Defective N-oxidation of sparteine in man: a new pharmacogenetic defect. Eur. J. Clin. Pharmacol. **16**, 183–187
3 Mahgoub, A., Idle, J. R., Dring, L. G., Lancaster, R. and Smith, R. L. (1977) Polymorphic hydroxylation of Debrisoquine in man. Lancet **2**, 584–586
4 Koymans, L., Vermeulen, N. P., van Acker, S. A., te Koppele, J. M., Heykants, J. J., Lavrijsen, K., Meuldermans, W. and Donne-Op den Kelder, G. M. (1992) A predictive model for substrates of cytochrome P450-debrisoquine (2D6). Chem. Res. Toxicol. **5**, 211–219
5 Smith, G., Stanley, L. A., Sim, E., Strange, R. C. and Wolf, C. R. (1995) Metabolic polymorphisms and cancer susceptibility. Cancer Surv. **25**, 27–65
6 McCann, S. J., Pond, S. M., James, K. M. and Le Couteur, D. G. (1997) The association between polymorphisms in the cytochrome P-450 2D6 gene and Parkinson's disease: a case-control study and meta-analysis. J. Neurol. Sci. **153**, 50–53
7 Ekins, S., de Groot, M. J. and Jones, J. P. (2001) Pharmacophore and three-dimensional quantitative structure activity relationship methods for modeling cytochrome P450 active sites. Drug Metab. Dispos. **29**, 936–944
8 Hiroi, T., Kishimoto, W., Chow, T., Imaoka, S., Igarashi, T. and Funae, Y. (2001) Progesterone oxidation by cytochrome P450 2D isoforms in the brain. Endocrinology **142**, 3901–3908
9 Niwa, T., Yabusaki, Y., Honma, K., Matsuo, N., Tatsuta, K., Ishibashi, F. and Katagiri, M. (1998) Contribution of human hepatic cytochrome P450 isoforms to regioselective hydroxylation of steroid hormones. Xenobiotica **28**, 539–547
10 Guengerich, F. P., Miller, G. P., Hanna, I. H., Martin, M. V., Leger, S., Black, C., Chauret, N., Silva, J. M., Trimble, L. A., Yergey, J. A. and Nicoll-Griffith, D. A. (2002) Diversity in the oxidation of substrates by cytochrome P450 2D6: lack of an obligatory role of aspartate 301-substrate electrostatic bonding. Biochemistry **41**, 11025–11034
11 Smith, G., Modi, S., Pillai, I., Lian, L. Y., Sutcliffe, M. J., Pritchard, M. P., Friedberg, T., Roberts, G. C. and Wolf, C. R. (1998) Determinants of the substrate specificity of human cytochrome P-450 CYP2D6: design and construction of a mutant with testosterone hydroxylase activity. Biochem. J. **331**, 783–792
12 Grace, J. M., Kinter, M. T. and Macdonald, T. L. (1994) Atypical metabolism of deprenyl and its enantiomer, (*S*)-(+)-*N*,alpha-dimethyl-*N*-propynylphenethylamine, by cytochrome P450 2D6. Chem. Res. Toxicol. **7**, 286–290
13 Ghahramani, P., Ellis, S. W., Lennard, M. S., Ramsay, L. E. and Tucker, G. T. (1997) Cytochromes P450 mediating the N-demethylation of amitriptyline. Br. J. Clin. Pharmacol. **43**, 137–144
14 Lin, L. Y., Di Stefano, E. W., Schmitz, D. A., Hsu, L., Ellis, S. W., Lennard, M. S., Tucker, G. T. and Cho, A. K. (1997) Oxidation of methamphetamine and methylenedioxymethamphetamine by CYP2D6. Drug Metab. Dispos. **25**, 1059–1064
15 Modi, S., Gilham, D. E., Sutcliffe, M. J., Lian, L. Y., Primrose, W. U., Wolf, C. R. and Roberts, G. C. (1997) 1-Methyl-4-phenyl-1,2,3,6-tetrahydropyridine as a substrate of cytochrome P450 2D6: allosteric effects of NADPH-cytochrome P450 reductase. Biochemistry **36**, 4461–4470
16 Yu, A., Dong, H., Lang, D. and Haining, R. L. (2001) Characterization of dextromethorphan O- and N-demethylation catalyzed by highly purified recombinant human CYP2D6. Drug Metab. Dispos. **29**, 1362–1365
17 Ellis, S. W., Hayhurst, G. P., Smith, G., Lightfoot, T., Wong, M. M., Simula, A. P., Ackland, M. J., Sternberg, M. J., Lennard, M. S., Tucker, G. T. and Wolf, C. R. (1995) Evidence that aspartic acid 301 is a critical substrate-contact residue in the active site of cytochrome P450 2D6. J. Biol. Chem. **270**, 29055–29058
18 Mackman, R., Tschirret-Guth, R. A., Smith, G., Hayhurst, G. P., Ellis, S. W., Lennard, M. S., Tucker, G. T., Wolf, C. R. and Ortiz de Montellano, P. R. (1996) Active-site topologies of human CYP2D6 and its aspartate-301 → glutamate, asparagine, and glycine mutants. Arch Biochem Biophys **331**, 134–140
19 Hanna, I. H., Kim, M. S. and Guengerich, F. P. (2001) Heterologous expression of cytochrome P450 2D6 mutants, electron transfer, and catalysis of bufuralol hydroxylation: the role of aspartate 301 in structural integrity. Arch. Biochem. Biophys. **393**, 255–261
20 Guengerich, F. P., Hanna, I. H., Martin, M. V. and Gillam, E. M. (2003) Role of glutamic acid 216 in cytochrome P450 2D6 substrate binding and catalysis. Biochemistry **42**, 1245–1253
21 Paine, M. J. I., McLaughlin, L. A., Flanagan, J. U., Kemp, C. A., Sutcliffe, M. J., Roberts, G. C. K. and Wolf, C. R. (2003) Residues glutamate-216 and aspartate-301 are key determinants of substrate specificity and product regiospecificity in cytochrome P450 2D6. J. Biol. Chem. **278**, 4021–4027
22 Kirton, S. B., Kemp, C. A., Tomkinson, N. P., St-Gallay, S. and Sutcliffe, M. J. (2002) Impact of incorporating the 2C5 crystal structure into comparative models of cytochrome P450 2D6. Proteins **49**, 216–231
23 Pritchard, M. P., Ossetian, R., Li, D. N., Henderson, C. J., Burchell, B., Wolf, C. R. and Friedberg, T. (1997) A general strategy for the expression of recombinant human cytochrome P450s in *Escherichia coli* using bacterial signal peptides: expression of CYP3A4, CYP2A6, and CYP2E1. Arch. Biochem. Biophys. **345**, 342–354
24 Pritchard, M. P., Glancey, M. J., Blake, J. A., Gilham, D. E., Burchell, B., Wolf, C. R. and Friedberg, T. (1998) Functional co-expression of CYP2D6 and human NADPH-cytochrome P450 reductase in *Escherichia coli*. Pharmacogenetics **8**, 33–42
25 Kunkel, T. A., Roberts, J. D. and Zakour, R. A. (1987) Rapid and efficient site-specific mutagenesis without phenotypic selection. Methods Enzymol. **154**, 367–382
26 Renaud, J. P., Peyronneau, M. A., Urban, P., Truan, G., Cullin, C., Pompon, D., Beaune, P. and Mansuy, D. (1993) Recombinant yeast in drug metabolism. Toxicology **82**, 39–52
27 Omura, T. and Sato, R. (1964) The carbon monoxide-binding pigment of liver microsomes. I. Evidence for its hemoprotein nature. J. Biol. Chem. **239**, 2370–2378
28 Sali, A. and Blundell, T. L. (1993) Comparative protein modelling by satisfaction of spatial restraints. J. Mol. Biol. **234**, 779–815
29 Jones, G., Willett, P. and Glen, R. C. (1995) Molecular recognition of receptor sites using a genetic algorithm with a description of desolvation. J. Mol. Biol. **245**, 43–53
30 Jones, G., Willett, P., Glen, R. C., Leach, A. R. and Taylor, R. (1997) Development and validation of a genetic algorithm for flexible docking. J. Mol. Biol. **267**, 727–748
31 Verdonk, M. L., Cole, J. C., Hartshorn, M. J., Murray, C. W. and Taylor, R. D. (2003) Improved protein–ligand docking using GOLD. Proteins **52**, 609–623
32 Clark, M., Cramer III, R. D. and Van Opdenbosch, N. (1989). J. Comp. Chem. **10**, 982–1012
33 Macdonald, T. L., Gutheim, W. G., Martin, R. B. and Guengerich, F. P. (1989) Oxidation of substituted *N,N*-dimethylanilines by cytochrome P-450: estimation of the effective oxidation–reduction potential of cytochrome P-450. Biochemistry **28**, 2071–2077
34 Smith, G., Stubbins, M. J., Harries, L. W. and Wolf, C. R. (1998) Molecular genetics of the human cytochrome P450 monooxygenase superfamily. Xenobiotica **28**, 1129–1165
35 Hayhurst, G. P., Harlow, J., Chowdry, J., Gross, E., Hilton, E., Lennard, M. S., Tucker, G. T. and Ellis, S. W. (2001) Influence of phenylalanine-481 substitutions on the catalytic activity of cytochrome P450 2D6. Biochem. J. **355**, 373–379
36 Williams, P. A., Cosme, J., Ward, A., Angove, H. C., Matak Vinkovic, D. and Jhoti, H. (2003) Crystal structure of human cytochrome P450 2C9 with bound warfarin. Nature (London) **424**, 464–468
37 Mancy, A., Broto, P., Dijols, S., Dansette, P. M. and Mansuy, D. (1995) The substrate binding site of human liver cytochrome P450 2C9: an approach using designed tienilic acid derivatives and molecular modeling. Biochemistry **34**, 10365–10375
38 Islam, S. A., Wolf, C. R., Lennard, M. S. and Sternberg, M. J. (1991) A three-dimensional molecular template for substrates of human cytochrome P450 involved in debrisoquine 4-hydroxylation. Carcinogenesis **12**, 2211–2219
39 Vaz, A. D. N., Roberts, E. S. and Coon, M. J. (1991) Olefin formation in the oxidative deformylation of aldehydes by cytochrome P-450. Mechanistic implications for catalysis by oxygen-derived peroxide. J. Am. Chem. Soc. **113**, 5886–5887
40 Haining, R. L., Jones, J. P., Henne, K. R., Fisher, M. B., Koop, D. R., Trager, W. F. and Rettie, A. E. (1999) Enzymatic determinants of the substrate specificity of CYP2C9: role of B′–C loop residues in providing the pi-stacking anchor site for warfarin binding. Biochemistry **38**, 3285–3292

Received 9 January 2004/13 February 2004; accepted 1 March 2004
Published as BJ Immediate Publication 1 March 2004, DOI 10.1042/BJ20040062